Spatiotemporal Pattern of Soil Respiration of Terrestrial Ecosystems in China: The Development of a Geostatistical Model and Its Simulation

GUIRUI YU,*,† ZEMEI ZHENG,‡ QIUFENG WANG,† YULING FU,† JIE ZHUANG,†,§ XIAOMIN SUN,† AND YUESI WANG‖

Synthesis Research Center of Chinese Ecosystem Research Network, Key Laboratory of Ecosystem Network Observation and Modeling, Institute of Geographic Sciences and Natural Resources Research, Chinese Academy of Sciences, 11A Datun Road, Chaoyang District, Beijing 100101, China, Department of Environmental Science and Technology, East China Normal University, Shanghai 200062, China, Department of Biosystems Engineering and Soil Science, Institute for a Secure and Sustainable Environment, Center for Environmental Biotechnology, The University of Tennessee, Knoxville, Tennessee 37996-4134, and Institute of Atmospheric Physics, Chinese Academy of Sciences, Beijing 100029, China

Received April 8, 2010. Revised manuscript received July 2, 2010. Accepted July 6, 2010.

Quantification of the spatiotemporal pattern of soil respiration (R_s) at the regional scale can provide a theoretical basis and fundamental data for accurate evaluation of the global carbon budget. This study summarizes the R_s data measured in China from 1995 to 2004. Based on the data, a new region-scale geostatistical model of soil respiration (GSMSR) was developed by modifying a global scale statistical model. The GSMSR model, which is driven by monthly air temperature, monthly precipitation, and soil organic carbon (SOC) density, can capture 64% of the spatiotemporal variability of soil R_s. We evaluated the spatiotemporal pattern of R_s in China using the GSMSR model. The estimated results demonstrate that the annual R_s in China ranged from 3.77 to 4.00 Pg C yr^{-1} between 1995 and 2004, with an average value of 3.84 $\pm$ 0.07 Pg C yr^{-1}, contributing 3.92%–4.87% to the global soil CO_2 emission. Annual R_s rate of evergreen broadleaved forest ecosystem was 698 $\pm$ 11 g C m^{-2} yr^{-1}, significantly higher than that of grassland (439 $\pm$ 7 g C m^{-2} yr^{-1}) and cropland (555 $\pm$ 12 g C m^{-2} yr^{-1}). The contributions of grassland, cropland, and forestland ecosystems to the total R_s in China were 48.38 $\pm$ 0.35%, 22.19 $\pm$ 0.18%, and 20.84 $\pm$ 0.13%, respectively.

1. Introduction

Soil respiration is a major process of carbon dioxide emission from terrestrial ecosystems to atmosphere (*1*). Thus, quantifying the spatiotemporal pattern of soil respiration (R_s) at the regional or continental scale is critical to establish an experimental and theoretical basis for accurate assessment of the global carbon budget. Three major approaches are available for estimating R_s at the regional scale. The inventory method multiplies the mean R_s rates of each land cover type by its area. Then, the total of the CO_2 emissions from different land covers is taken as the total R_s (*2*). The second method calculates the R_s and its spatiotemporal variability using a process-based model (*3*). The third uses geostatistical model of R_s, which is constructed based on the relationships between environmental variables and measured soil carbon flux (*4, 5*).

Each method has weakness and uncertainties. The inventory method is limited by the quality and the spatiotemporal representativeness of measured R_s data. Poor data can result in infinite uncertainty on R_s estimates at the regional scale. The process-based R_s model can simulate the spatial patterns and also predict the long-term dynamics of ecosystem R_s (*6*). However, the process-based R_s model has complicated structure in coupling with soil–plant–atmosphere processes. It is thus difficult to evaluate the rationality of the estimated results when considerably large uncertainty exists in the spatial representativeness of model parameters. Relatively, the geostatistical R_s model has simple structure, sound parameterization method, and reasonable results (*4, 7*), though it cannot predict R_s changes with climate, nitrogen deposition, etc. It is usually built on the relationships between in situ R_s rates and environmental variables, such as temperature, precipitation, and leaf area index (LAI). In addition, the geostatistical model can validate the process-based R_s model by providing independent data on soil CO_2 emissions. Therefore, the geostatistical R_s model is most widely used in the quantification of spatiotemporal variability of R_s at regional scale (*4*).

Progress has been made on the research of R_s quantification in China over the past decade. Fang et al. estimated the annual R_s of terrestrial ecosystems in China using the inventory method (*8*). Zhou et al. inversely simulated the spatial pattern of heterotrophic respiration using remote sensing data and climatic data (*9*). Cao et al. evaluated the spatiotemporal pattern of heterotrophic respiration of Chinese terrestrial ecosystems based on a process-based model (i.e., CEVSA model) (*3*). Continuous measurements of R_s over typical forestland, grassland, and cropland ecosystems in China provide abundant data for evaluating the spatiotemporal variability of R_s in China and its environmental constraints as well as the region-specific behaviors of geostatistical model of R_s (*10, 11*). By synthesizing the measured R_s data of ChinaFLUX and the R_s data from the published literature, Zheng et al. found that the spatial variability of Q_{10} of R_s in China was determined by soil temperature, soil organic carbon (SOC) density, and ecosystem type, and that the spatial pattern of Q_{10} could be described as an exponential function of soil temperature (*12*). Based on the R_s database of ChinaFLUX, Zheng et al. tested the applicability of a global-scale R_s model presented by Raich (*5*) (hereafter called TP model) to quantification of the spatiotemporal variability of R_s of forest ecosystems in China (*13*). In their study, the TP model was modified into an empirical statistical model, which is driven by monthly air temperature, monthly precipitation, and SOC density (*13*).

This study summarizes the R_s data set of the ChinaFLUX and the published data in China over the past decade. The objectives were (1) to test whether the model by Raich et al. (*5*) could be used to describe the spatiotemporal variation of R_s in China and, if not, how to modify it; (2) to construct

* Corresponding author fax: (86)10-64889432; e-mail: yugr@igsnrr.ac.cn.

† Synthesis Research Center of Chinese Ecosystem Research Network, Key Laboratory of Ecosystem Network Observation and Modeling, Institute of Geographic Sciences and Natural Resources Research, Chinese Academy of Sciences.

‡ East China Normal University.

§ The University of Tennessee.

‖ Institute of Atmospheric Physics, Chinese Academy of Sciences.

10.1021/es100979s

Published on Web 07/19/2010

a geostatistical model of R_s (GSMSR) driven by air temperature, precipitation, and SOC density; and (3) to evaluate the temporal (seasonal and interannual) and spatial variability of R_s in China from 1995 to 2004 and the contribution of R_s in China to the global soil carbon emission.

2. Data Sources and Model Development

2.1. Collection and Integration of R_s Measurement Data in China. In this study, an R_s database of China was established by synthesizing the R_s data set of ChinaFLUX and those published in approximately 200 papers in the literature. To ensure the comparability of the measured R_s, we only selected the data measured using static chamber/GC method and static/dynamic chamber/IRGA method (*13*). The selected R_s data sets were built at both monthly and annual scales.

The monthly R_s were compiled in the same way as used by Raich et al. (*5*). All available R_s observations were averaged per month and ecosystem, then R_s data in the same month of different years were averaged to obtain monthly mean R_s. Note that the monthly R_s data derived from R_s equations in the literature were not included in our database. In total, 390 monthly R_s data observed at 21 sites and 40 ecosystems were obtained (Figure 1a). The annual R_s data were either collected from the literature or estimated from the linear interpolation of collected daily R_s. The annual R_s values of different years were averaged for each ecosystem. A total of 50 annual R_s data for 26 sites were collected (Figure 1b).

2.2. Data Spatialization and Processing of Environmental Variables. To quantify the spatiotemporal pattern of R_s (1 km × 1 km, monthly scale) and the variables driving the model, we spatialized the data of the following environmental variables. Grid monthly air temperature and monthly precipitation (1 km × 1 km) were interpolated from climate data of 678 meteorological sites using a specially designed interpolation package for meteorological data ANUSPLIN 3.1 (*14*). Grid SOC density data at a depth of 20 cm (1 km × 1 km) were obtained based on the interpolation from the 1:4000000 SOC density vector data (*15*). Grid land cover data (1 km × 1 km) were derived by distilling China from the global grid land cover data (*16*).

2.3. Construction of the Geostatistical R_s Model of China. *(1) Test of the Capability of a Global-Scale R_s Model.* The R_s equations based on Lloyd and Talyor (*17*) include the van't Hoff, Arrhenius, and Lloyd−Taylor equations. We compared the three equations, and found that no significant difference existed among the results, therefore, we used the van't Hoff equation to quantify the dependence of R_s on temperature (eq 1) because the majority of our studied ecosystems, which were free of the stresses of water and other environmental factors, had a fixed temperature sensitivity.

$$R_s = R_0 e^{bt} \tag{1}$$

where R_s is the instantaneous soil respiration rate (μmol m^{-2} s^{-1}), R_0 is soil respiration rate at a reference temperature of 0 °C (μmol m^{-2} s^{-1}), and t is actual air temperature (°C).

The following two equations were used to analyze the response of monthly R_s to temperature and precipitation, respectively (*5*),

$$R_{s,\mathrm{monthly}} = R_0 e^{QT} \tag{2}$$

$$R_{s,\mathrm{monthly}} = P_0 + P/(P + K) \tag{3}$$

where $R_{s,\mathrm{monthly}}$ is monthly mean R_s rate (g C m^{-2} d^{-1}), T is monthly air temperature, P is monthly precipitation, Q is temperature sensitivity of R_s, and P_0 and K are regression parameters.

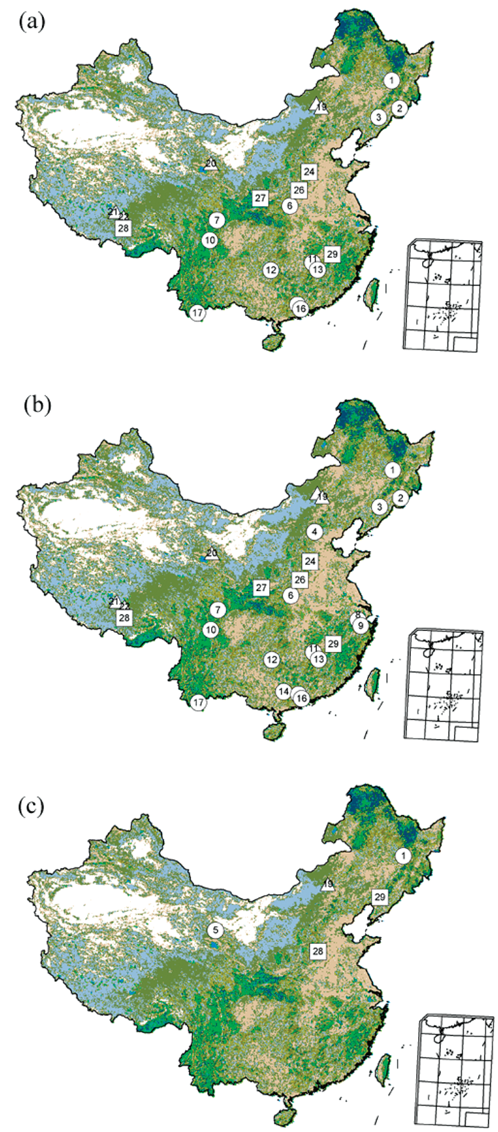

FIGURE 1. Spatial distribution of R_s measurement sites: (a) monthly R_s; (b) annual R_s; (c) R_s data for validating the capability of GSMSR for explaining the seasonal variation of R_s. ○: Forest; Δ: Grassland; □: Cropland. Forest sites name (abbrev.): 1, Maoershan (MR); 2, Changbaishan (C); 3, Qingyuan (Q); 4, Donglingshan (DL); 5, Qilianshan (QL); 6, Baotianman (B); 7, Miyaluo (M); 8, Hangzhou (HZ); 9, Zhuji (Z); 10, Gonggashan (G); 11, Dagangshan (D); 12, Huitong (HT); 13, Qianyanzhou (QY); 14, Heishiding (HSD); 15, Dinghushan (DH); 16, Heshan (HS); 17, Xishuangbanna (XS). Grassland sites name (abbrev.): 18, Xilinhot (XL); 19, Xilinhe (X); 20, Haibei (H); 21, Bange (BG); 22, Damxung (DX). Cropland sites name (abbrev.): 23, Shenyang (S); 24, Yucheng (Y); 25, Anyang (A); 26, Fengqiu (F); 27, Yangling (YL); 28, Lasa (L); 29, Yingtan (YT).

Raich et al. (*5*) presented TP model (eq 4) to evaluate the impacts of temperature and precipitation on the spatiotemporal pattern of the global R_s,

$$R_{s,\mathrm{monthly}} = R_0 e^{QT} P/(P + K) \tag{4}$$

where the definitions of variables and parameters are the same as those in above equations. The values of parameters are $R_0 = 1.250$, $Q = 0.055$, and $K = 4.25$ (*5*).

In this study, the ability of TP model for estimating the spatiotemporal variability of $R_{s,\mathrm{monthly}}$ was tested using the above parameter values and the collected 333 monthly mean R_s data. The results show that the coefficient of determination

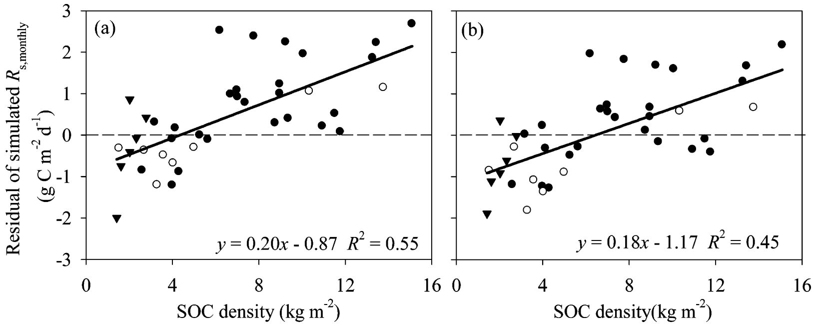

FIGURE 2. Relationship between SOC density at a depth of 20 cm and residual of simulated $R_{s,monthly}$: (a) TP; (b) TP2; ●: forest; ○: grassland; ▼: cropland. Residuals of simulated $R_{s,monthly}$ values were averaged within each ecosystem.

between the simulated and measured R_s values was only 0.37 with considerable systematic error. Therefore, TP model was reparameterized using the collected data. The model modified with new parameter values ($R_0 = 1.740$, $Q = 0.029$, $K = 0.911$) is referred to as TP2 model. However, TP2 model could only explain 40% of the spatiotemporal variability of the monthly mean R_s showing limited improvement in the systematic error (Figure S1).

(2) Construction of a New R_s Model. Neither the original TP model nor the reparameterized TP model (i.e., TP2 model) could well explain the spatial variability of $R_{s,monthly}$ in China. When comparing the averages of the measured and predicted $R_{s,monthly}$ of the same ecosystem, large systematic errors of TP and TP2 models still existed, partly due to their insufficient capture of the variability of $R_{s,monthly}$ of different types of ecosystems at the same site.

Figure 2 illustrates the residual of simulated $R_{s,monthly}$. The strong correlation between the residual and SOC density suggests that SOC density was an additional factor controlling the spatial variability of $R_{s,monthly}$.

Based on the above results, we propose a new R_s model (eq 5) by modifying the parameter R_0 in eq 4 as a linear function of SOC density. The resulting model is

$$R_{s,monthly} = (R_{Ds=0} + MDs)e^{QT}(P + P_0)/(P + K) \qquad (5)$$

where D_S is SOC density at a soil depth of 20 cm, $R_{Ds=0}$ is the $R_{s,monthly}$ rate when the SOC density is zero, and M is parameter. The TP model has the implicit assumption of "zero-precipitation−zero-respiration", which is actually not the scenario of natural processes. In eq 5, taking an approach similar to that by Reichstein et al. (*7*), we added a parameter P_0 to the model for taking into account the capability of water retention in soil.

Furthermore, Zheng et al. (*12*) found that the spatial variability of Q in China could be described by an exponential function of air temperature

$$Q = \ln \alpha e^{\beta T} \qquad (6)$$

where α and β are fitted parameters. By putting the eq 6 into eq 5, a new geostatistical model of soil respiration (GSMSR) can be obtained (eq 7) as follows

$$R_{s,monthly} = (R_{Ds=0} + MDs)e^{\ln \alpha e^{\beta T} T/10}(P + P_0)/(K + P) \qquad (7)$$

In this study, 333 R_s data selected randomly from a total of 390 collected data were used for parametrization of the GSMSR model. The resulting parameters were $R_{Ds=0} = 0.588$, $M = 0.118$, $\alpha = 1.83$, $\beta = -0.006$, $P_0 = 2.972$, and $K = 5.657$.

2.4. Model Validation. Figure 3a and b demonstrates the ability of GSMSR to explain the variability of monthly mean R_s. Comparison of the measured and the simulated $R_{s,monthly}$ shows that the GSMSR model explains 64% of the seasonal variability of $R_{s,monthly}$, 58% of the variability of R_s among different ecosystems at the same site, and 51% of the variability of annual R_s (Figure 3c).

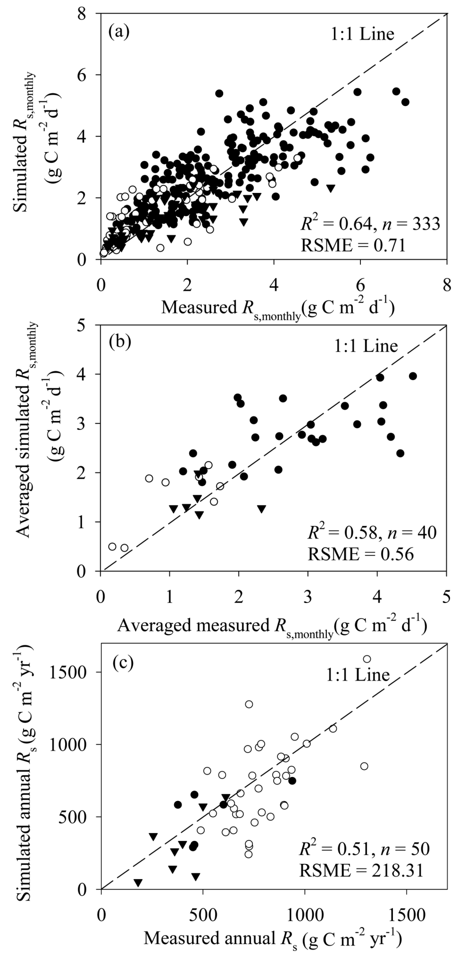

FIGURE 3. Comparison between measured R_s and simulated R_s of GSMSR model (●: forest; ○: grassland; ▼: cropland). (a) Data were monthly mean R_s rates; (b) data from the same ecosystem in (a) were averaged; (c) data from the same ecosystem in (a) were aggregated to annual values.

The GSMSR model was also validated with 57 R_s data that were not used in the model parametrization. These data were measured at four forestland ecosystems (MR1 and MR2 in Maoershan, QL1 and QL2 in Qilianshan), three grassland ecosystems (X4, X5, and X6 in Xilinhe), and two cropland ecosystems (S in Shenyang, AY in Anyang) (Figure 1c). The results demonstrate that the GSMSR model could well describe the seasonal dynamics of R_s of different terrestrial ecosystems (Figure S2). The measured values were significantly correlated with the estimated ($R^2 = 0.68$) (Figure S3).

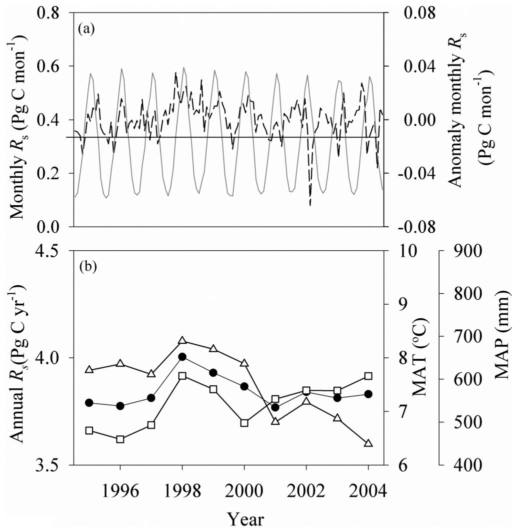

FIGURE 4. Seasonal variability of monthly R_s (bold line) and anomaly monthly R_s (dashed line) from 1995 to 2004 (a); and the interannual variability of annual R_s (●), MAT (□, mean annual air temperature), and MAP (△, mean annual precipitation) (b).

2.5. Boundaries of the GSMSR Parameters. The GSMSR model was driven by the spatialized environmental variables at monthly scale, and the parameters were determined empirically. If the values of environmental variables exceed the boundary condition of parameterization, the estimated result might bring discrepancy. Since SOC density at a soil depth of 20 cm in China mostly ranged from 0 to 15.09 kg m^{-2}, R_s rate was set to be unchanged if SOC density reached 15.09 kg m^{-2} in this study. Monthly air temperature for model parametrization ranged from −15.96 to 30.96 °C. Therefore, we assumed that R_s rate was zero and the maximum when T was lower than −15.96 °C and higher than 30.96 °C, respectively.

3. Analysis of the Spatiotemporal Pattern of R_s

3.1. Spatial Pattern of R_s in China and Its Interannual Variation. Using the GSMSR model, we obtained the spatial pattern of $R_{s,monthly}$ in China. The $R_{s,monthly}$ values were then aggregated to the annual R_s rates. The mean annual R_s from 1995 to 2004 increased along the direction from the northwest to the southeast of China with the values varying from 51 to 1592 g C m^{-2} yr^{-1} (Figure S4). The annual soil CO_2 emission in China ranged from 3.77 to 4.00 Pg C yr^{-1} during the same period, while the anomaly monthly R_s (the deviation from the 1995−2004 mean) varied from −0.064 to 0.035 Pg C mon^{-1} (Figure 4a). The annual R_s rates in the years with abundant precipitation (e.g., 1999 and 2000), higher air temperature (e.g., 2004), or both (e.g., 1998) were obviously larger than those in other years (Figure 4a, b).

3.2. Spatial Pattern of R_s along Longitude and Latitude Gradients. Figure 5 shows the mean annual R_s along the longitude and latitude gradients at the bins of 5°. Mean annual R_s first decreased and then increased with increasing latitude. The highest value (i.e., 827 ± 33 g C m^{-2} yr^{-1}) occurred in latitudes ranging from 15° to 20° N. The lowest value (286 ± 7 g C m^{-2} yr^{-1}) occurred from 35° to 40° N. As the longitude increases from 70° to 135° E, the annual R_s increased until 110−115° E following with a trough between 120° and 125° E. Specifically, the annual R_s rates stabilized at 236 ± 88 to 249 ± 105 g C m^{-2} yr^{-1} in the area from 70° to 90° E. An increase to the maximum of 550 ± 186 g C m^{-2} yr^{-1} occurred from 110° to 115° E with slight decline between 120° and 125° E.

3.3. Spatial Pattern of R_s along the Elevation Gradient. Figure 6 illustrates that the annual R_s varied significantly along the elevation gradient. The annual R_s decreased from

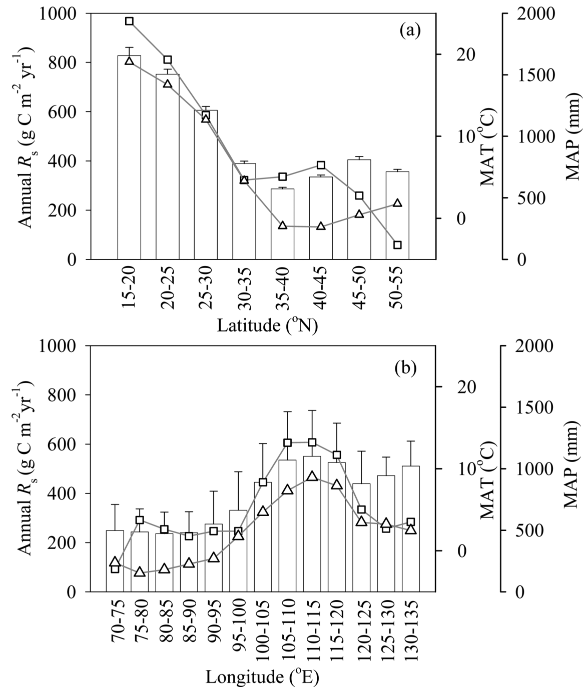

FIGURE 5. Annual R_s rates (column), MAT (□), and MAP (Δ) along latitude (a) and longitude (b) gradients.

585 ± 154 to 422 ± 183 g C m^{-2} yr^{-1} when the altitude increased from 0 to 1000 m, where the terrain was either plain or mountainous. However, the annual R_s increased from 365 ± 152 to 417 ± 159 g C m^{-2} yr^{-1} as the elevation of alpine terrain increased from 1000 to 2000 m. Similarly, the annual R_s rates increased from 333 ± 156 to 426 ± 158 g C m^{-2} yr^{-1} when the elevation on the Tibetan-Plateau terrain increased from 2000 to 4000 m. In contrast, significant decrease was observed at elevations exceeding 4000 m. For instance, the R_s value decreased from 318 ± 138 to 138 ± 65 g C m^{-2} yr^{-1} when the elevation increased from 4000 to 8000 m.

3.4. Seasonal Dynamics of R_s along the Latitude and Longitude Gradients. Figure 7 shows the seasonal dynamics of monthly R_s along the latitude and longitude gradients from 1994 to 2005. The monthly R_s at different latitude gradients followed the seasonal pattern of air temperature. However, the seasonal amplitude of monthly R_s varied with latitude. In the northern area (40° to 55° N), the seasonal amplitude of monthly R_s at high latitude was larger than that at low latitude mainly due to the large change in air temperature. Within the latitudes from 35° to 40° N, the seasonal amplitude of monthly R_s remained the smallest. Likewise, the seasonal dynamics of monthly R_s at different longitude gradients were in agreement with the seasonal pattern of temperature. The seasonal amplitude of R_s increased with increasing longitude from 70° to 135° E.

3.5. R_s of Different Land Cover Types. The mean annual soil CO_2 emission from 1995 to 2004 in China was 3.84 ± 0.07 Pg C yr^{-1}. The soil CO_2 emission from cropland (22.17 ± 0.18%) contributed most to the total emission, whereas deciduous needle-leaved forest contributed least (0.20 ± 0.01%, Table 1). In terms of annual soil CO_2 emission, the evergreen broad-leaved forest was the highest (698 ± 11 g C m^{-2} yr^{-1}), in contrast to the lowest from bare land (238 ± 9 g C m^{-2} yr^{-1}). The R_s rates of forestland were generally larger than those of cropland and grassland. The interannual R_s variation of deciduous needle-leaved forest was the largest (CV = 3.14%) and that of evergreen broad-leaved forest was the smallest (CV = 1.61%). The contributions of soil CO_2 emission from forestland, cropland, and grassland ecosystems to the total R_s in China were 48.38 ± 0.35%, 22.17 ± 0.18%, and 20.83 ± 0.13%, respectively.

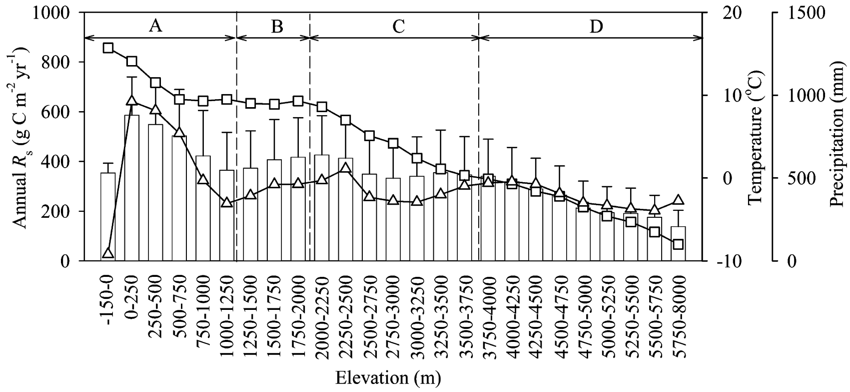

FIGURE 6. Annual R_s rates (column), MAT (□) and MAP (Δ) along elevation gradient (A: zone with the terrain was always plain or hill; B: zone with the terrain was alpine; C: zone with the terrain was Tibetan-Plateau; D: zone with the elevation exceeded 4000 m).

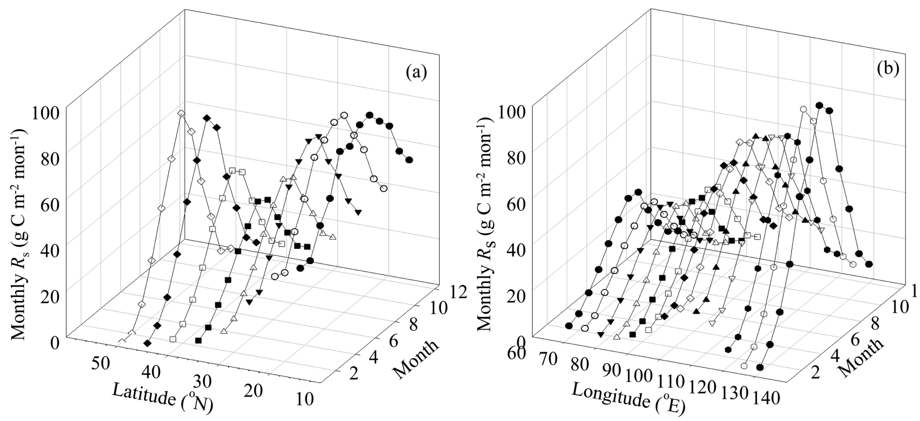

FIGURE 7. Seasonal dynamics of monthly R_s along latitude (a) and longitude (b) gradients.

TABLE 1. Annual R_s in Terms of Land Cover Types

land cover type	area (10^4 km^2)	annual R_s (Pg C)	CV (%)	contribution (%)	R_s rate (g C m^{-2} yr^{-1})
evergreen needle-leaved forest	36.61	0.20	2.08	5.17	542
evergreen broadleaved forest	3.66	0.03	1.61	0.67	698
deciduous needle-leaved forest	2.35	0.01	3.14	0.20	335
deciduous broadleaved forest	10.16	0.06	2.53	1.44	546
mixed forest	21.63	0.10	2.24	2.48	440
woodland	77.74	0.42	2.04	10.88	537
wooded grassland	106.53	0.60	2.03	15.50	559
closed shrubland	10.22	0.04	2.25	0.94	353
open shrubland	200.66	0.49	2.49	12.69	243
grassland	168.51	0.74	1.97	19.25	439
cropland	153.53	0.85	2.13	22.17	555
bare	138.90	0.33	2.18	8.62	238
total	930.50	3.84	1.92	100.0	

TABLE 2. Contribution of R_s in China to the Global Carbon Balance

	R_s (Pg C yr^{-1})				area (10^4 km^2)[a]				
region	total	forest	grassland	cropland	total	forest[b]	grassland [c]	cropland	SOC pool (Pg C)
China	3.84	0.82	1.87	0.85	930.50	152.15	485.92	153.53	89.14[d]
	80.40[f]	46.12	22.03	8.08	14315.50	5864.90	4680.40	1298.55	
global	98.00[g]								1220−1576[e]
contribution (%)	3.92−4.78	1.78	8.49	10.52	6.50	2.59	10.38	11.82	5.66−7.31

[a] The area was obtained based on the land cover data except polar ice and rock land in Hansen et al. (*18*). [b] The land cover types from 1 to 6 in Hansen et al. (*18*) were included. [c] The land cover types from 7 to 10 in Hansen et al. (*18*) were included. [d] Yu et al. (*15*). [e] Tarnocai et al. (*19*). [f] Raich et al. (*5*). [g] Bond-Lamberty and Thomson (*20*).

3.6. Contribution of R_s in China to the Global Carbon Budget. Table 2 shows the contribution of R_s in China to the global carbon budget from 1995 to 2004. The R_s in China accounted for 3.92%−4.78% of the global soil CO_2 emission, which was lower than the ratio of SOC pool in China to that of the global (5.66%−7.31%). The contributions of R_s of forestland, cropland, and grassland ecosystems in China to the global total R_s were 1.78%, 10.52%, and 8.49%, respectively.

TABLE 3. Comparison of Evaluation Results of R_s from Different Models

model	period	climatic data/spatial resolution	R_s (Pg C yr^{-1})	reference
GSMSR	1995−2004	interpolated from climate data of sites in China/1 × 1 km^2	3.84	this study
TP[a]	1980−1994	interpolated from climate data of sites of global/0.5° × 0.5°	3.76	Raich et al. (*5*)
TP[b]	1995−2004	interpolated from climate data of sites in China/1 × 1 km^2	3.51	this study
CEVSA	1980−2000	interpolated from climate data of sites in China/0.5° × 0.5°	4.82 (3.02[c])	Cao et al. (*3*)
AVIM2	1981−2000	PRECIS/50 × 50 km^2	4.43 (2.84[c])	Ji et al. (*22*)

[a] China data were distilled from global data calculated by Raich et al. (*5*). [b] The evaluation result of TP model (original parameters in Raich et al. (*5*)) with the climatic data of China. [c] Heterotrophic respiration (R_h), the R_s values were estimated from function: $\mathrm{Ln}(R_h) = 1.22 + 0.73\mathrm{Ln}(R_s)$ (*21*).

4. Discussion

4.1. Modification of Geostatistical R_s Model. The geostatistical R_s model can provide independent soil CO_2 emissions data for validating the process-based model (*4*). However, the global scale geostatistical R_s model needs reparameterization or modification in structure when it is used at a regional scale because the factors determining R_s vary with spatial scales.

The TP model presented by Raich et al. (*5*) is suitable for modeling R_s at the global scale. However, the model could not well explain the variability of R_s in China even if it was reparameterized with R_s data in China. In this study, GSMSR was developed on the basis of TP model. The modifications include (1) the reference R_s rate is expressed as a linear function of SOC density in consideration of the effect of SOC density on R_s (*13*), (2) temperature sensitivity of R_s (Q) is modified as an exponential function of temperature (i.e., $\ln\alpha e^{\beta T}$) (*12*), and (3) a parameter P_0 considering soil−water regime is introduced into the model (*7*). GSMSR can explain 64% of the spatiotemporal variability of R_s in China, much better than the behaviors of TP and TP2 models. The results suggest that the GSMSR model is suitable for evaluating the annual R_s and the seasonal variability of R_s of different ecosystems in China.

4.2. Comparison of R_s Evaluation by Different Models. Table 3 compares the R_s rates estimated by different models. The results of the GSMSR model fell within the results of other models. The mean annual R_s simulated by GSMSR was 3.84 Pg C yr $^{-1}$ from 1995 to 2004. This value was slightly larger than the estimation by Raich et al. (*5*) and by the TP model with the climatic data in China but smaller than the results of two process-based R_s models: CEVSA model (*3*) and AVIM2 model (*22*). We attribute such differences to the variations of spatial and temporal resolutions of environmental variables, modeling periods, and data used in the parametrization of models.

The GSMSR model is more accurate than other models in R_s simulation and estimation, but it may have two uncertainties that need verification. First, model parametrization requires more data for cropland ecosystems than for forestland and grassland ecosystems. As a result, the model applicability may vary with ecosystem types. Second, the model might have a certain limitation in spatial representativeness because most of the sites for model validation were located in the east of China. Testing based on the measurements in other areas would help clarify the potential of spatial representativeness of the model.

4.3. Spatiotemporal Pattern of R_s in China. The spatial patterns of R_s variation along latitude, longitude, and elevation gradients were correlated to the spatial patterns of air temperature, vegetation types, and SOC density. Along the latitude gradient, the ecosystems in the south of China had the largest soil CO_2 emission due to the high temperature (Figure 5a). Temperature was low in north China, but the annual R_s rates were still larger than those in central China (Figure 5a), chiefly because most ecosystems in this area at high latitudes were boreal forest ecosystems, and rich in SOC (respiration substrate) (*23*). The increase in R_s rates with longitude (Figure 5b) was due to the low vegetation coverage in west China. In general, the decrease in R_s in the area with high longitude was attributed to the land coverage by boreal and temperate forest ecosystems (Figure 5b). Temperature was the major factor controlling the temporal variation of R_s at the seasonal scale. This is why the seasonal dynamics of monthly R_s along latitude and longitude gradients were similar to that of temperature (Figure 7). Besides, the areas covered by forest ecosystems with high SOC density exhibited a sharp increase in soil CO_2 emission in summer (*12*). As a result, the seasonal amplitude of monthly R_s in northern China was larger than that in other areas (Figure 7b). Further study is needed to distinguish the effect of longitude/latitude and elevation.

Acknowledgments

This study was jointly funded by NSFC (30590381, 30700110, 30800151), Key Project of Chinese National Programs for Fundamental Research and Development from MOST (2010CB833500), Innovation Program of the CAS (KZCX2-YW-432), and the Fundamental Research Funds for the Central Universities (78210031).

Supporting Information Available

Additional figures.This material is available free of charge via the Internet at http://pubs.acs.org.

Literature Cited

(1) Davidson, E. A.; Janssens, I. A.; Luo, Y. Q. On the variability of respiration in terrestrial ecosystems: moving beyond Q_{10}. *Global Change Biol.* **2006**, *12*, 154–164.

(2) Raich, J. W.; Schlesinger, W. H. The global carbon dioxide flux in soil respiration and its relationship to vegetation and climate. *Tellus* **1992**, *44B*, 81–99.

(3) Cao, M. K.; Prince, S. D.; Li, K. R.; Tao, B.; Small, J.; Shao, X. M. Response of terrestrial carbon uptake to climate interannual variability in China. *Global Change Biol.* **2003**, *9*, 536–546.

(4) Raich, J. W.; Potter, C. S. Global patterns of carbon dioxide emissions from soils. *Global Biogeochem. Cycles* **1995**, *9*, 23−36.

(5) Raich, J. W.; Potter, C. S.; Bhagawai, D. Interannual variability in global soil respiration, 1980−94. *Global Change Biol.* **2002**, *8*, 800–812.

(6) Cramer, W.; Bondeau, A.; Woodward, F. I.; Prentice, I. C.; Betts, R. A.; Brovkin, V.; Cox, P. M.; Fisher, V.; Foley, J.; Friend, A. D.; et al. Global response of terrestrial ecosystem structure and function to CO_2 and climate change, results from six dynamic global vegetation models. *Global Change Biol.* **2001**, *7*, 357–373.

(7) Reichstein, M.; Rey, A.; Freibauer, A.; Tenhunen, J.; Valentini, R.; Banza, J.; Casals, P.; Cheng, Y.; Grünzweig, J. M.; Irvine, J.; et al. Modeling temporal and large-scale spatial variability of soil respiration from soil water availability, temperature and vegetation productivity indices. *Global Biogeochem. Cycles* **2003**, *17*, 1104; doi:10.1029/2003GB002035.

(8) Fang, J. Y.; Liu, G. H.; Xu, S. L. Carbon pool of terrestrial ecosystems in China. In *Hotpoints for Modern Ecology Research*; Wang, R. S., Ed; China Science and Technology Press: Beijing, 1996.

(9) Zhou, T.; Shi, P. J.; Sun, R.; Wang, S. Q. The impacts of climate change on net ecosystem production in China (In Chinese). *Acta Geograph. Sin.* **2004**, *59*, 357–365.

(10) Wang, Y. S.; Wang, Y. H. Quick measurement of CH_4, CO_2 and N_2O emission from a short-plant ecosystem. *Adv. Atmos. Sci.* **2003**, *20*, 842–844.

(11) Yu, G. R.; Fu, Y. L.; Sun, X. M.; Wen, X. F.; Zhang, L. M. Recent progress and future directions of ChinaFLUX. *Sci. China Ser. D* **2006**, *49* (Supp. II), 1–23.

(12) Zheng, Z. M.; Yu, G. R.; Fu, Y. L.; Wang, Y. S.; Sun, X. M.; Wang, Y. H. Temperature sensitivity of soil respiration is affected by prevailing climatic conditions and soil organic carbon content: a trans-China based case study. *Soil Biol. Biochem.* **2009**, *41*, 1531–1540.

(13) Zheng, Z. M.; Yu, G. R.; Sun, X. M.; Li, S. G.; Wang, Y. S.; Wang, Y. H.; Fu, Y. L.; Wang, Q. F. Spatio-temporal variability of soil respiration of forest ecosystems in China: Controlling factors and evaluation model. *Environ. Manage.* **2010**; doi:10.1007/s00267-010-9509-z.

(14) Hutchinson, M. F. Interpolation of rainfall data with thin plate smoothing splines- Part I: Two dimensional smoothing of data with short range correlation. *J. Geogr. Inform. Decis. Anal.* **1998**, *2*, 139–151.

(15) Yu, D. S.; Shi, X. Z.; Sun, W. X.; Wang, H. J.; Liu, Q. H.; Zhao, Y. C. Estimation of China soil organic carbon storage and density based on 1:1000000 soil database (In Chinese). *Chin. J. Appl. Ecol.* **2005**, *16*, 2279–2283.

(16) Hansen, M. C.; Defries, R. S.; Townshend, J. R. G.; Sohlberg, R. Global land cover classification at 1 km spatial resolution using a classification tree approach. *Int. J. Remote Sens.* **2000**, *21*, 1331–1364.

(17) Lloyd, J.; Taylor, J. A. On the temperature dependence of soil respiration. *Funct. Ecol.* **1994**, *8*, 315–323.

(18) Hansen, J. E.; Ruedy, R.; Sato, M.; Imhoff, M.; Lawrence, W.; Easterling, D.; Peterson, T.; Karl, T. A closer look at United States and global surface temperature change. *J. Geophys. Res.* **2001**, *106*, 23947–23963; doi:10.1029/2001JD000354.

(19) Tarnocai, C.; Canadell, J. G.; Schuur, E. A. G.; Kuhry, P.; Mazhitova, G.; Zimov, S. A. Soil organic carbon pools in the northern circumpolar permafrost region. *Global Biogeochem. Cycles* **2009**, *23*, GB2023; doi:10.1029/2008GB003327.

(20) Bond-Lamberty, B.; Thomson, A. Temperature-associated increases in the global soil respiration record. *Nature* **2010**, *464*, 579–582.

(21) Bond-Lamberty, B.; Wang, C.; Gower, S. T. Net primary production and net ecosystem production of a boreal black spruce wildfire chronosequence. *Global Change Biol.* **2004**, *10*, 473–487.

(22) Ji, J. J.; Huang, M.; Li, K. R. Prediction of carbon exchanges between China terrestrial ecosystem and atmosphere in 21st century. *Sci. China Ser. D* **2008**, *51*, 885–898.

(23) Wang, S. Q.; Zhou, C. H.; Li, K. R.; Zhu, S. L.; Huang, F. H. Analysis on spatial distribution characteristics of soil organic carbon reservoir in China (In Chinese). *Acta Geograph. Sin.* **2000**, *55*, 533–544.

ES100979S